

## Impurity transport studies in multiple helicity and enhanced confinement QSH regimes in RFX-mod

S. Menmuir, L. Carraro, A. Fassina, A. Alfier, F. Auriemma, P. Franz, M.E. Puiatti,  
M. Valisa

*Consorzio RFX, Associazione Euratom-ENEA sulla Fusione, Padova, Italy*

The most recent impurity transport studies in RFX-mod are presented. Results from enhanced confinement quasi-single helicity (QSH) and multiple helicity (MH) are compared. The transport parameters are determined by comparing a 1-dimensional collisional radiative simulation with experimental spectroscopic data. Transport parameters obtained for Ni particles injected by the laser blow-off method are described and discussed in relation to results from Ne injection and previous studies.

**Introduction** The high plasma current discharges ( $I_p \geq 1\text{MA}$ ) in the reversed field pinch device RFX-mod are characterised by intermittent QSH phases, marked by the presence of a thermal island, that occupy a significant fraction of the discharge. There is a strong increase of the electron temperature ( $T_e$ ) in the QSH island and steep gradients consistent with internal transport barriers [1].

A series of experiments were carried out injecting Ni into the RFX-mod plasma through the laser blow-off (LBO) technique. Signals from a number of spectroscopic diagnostics were monitored, including Ni XVII ( $249\text{\AA}$ ) and Ni XVIII ( $292\text{\AA}$ ) line emission and soft X-ray (SXR) time evolution and radial brightness profile reconstructions – normalised to a pre-LBO profile to remove the C and O contribution (assumed constant during the LBO).

In order to estimate the impurity (Ni) diffusion coefficient  $D$  and pinch velocity  $v$ , the experimental signals during the LBO pulse have been simulated with a 1-dimensional collisional-radiative model [2]. Experimental electron temperature and density are input to the code along with an influx time behaviour

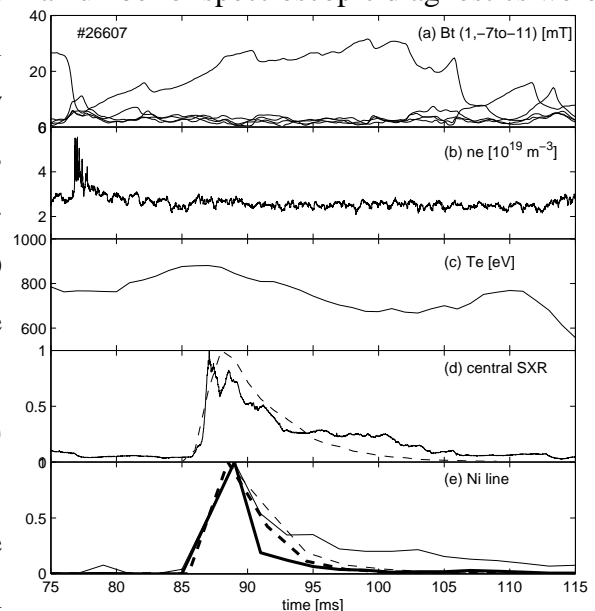


Figure 1: Discharge #26607 (1.55MA, LBO at 85ms): (a)  $B_t$   $m=1$ ,  $n=-7$  to  $-11$ ; (b)  $n_e$ ; (c)  $T_e$ ; (d) central chord SXR and simulation (dashed); (e) NiXVII  $249\text{\AA}$  (thick) and NiXVIII  $292\text{\AA}$  line emission with respective simulations (dashed).

based on the Thomson spectrometer signal on a chord looking to the LBO port. The simulation is repeated with different  $D$  and  $v$  radial profiles in order to find a reasonable reproduction of the experimental data.

**Ni transport in QSH** Figure 1 depicts a LBO during the flat-top phase of a long-lasting QSH period, allowing the whole Ni particle evolution to occur before the QSH crash. The code is able to well reproduce the time evolution of the Ni line and central chord SXR emissions. Figure 2 demonstrates that, in the simulation and experiment, immediately after LBO the SXR profiles are hollow and then return to being centrally peaked. The determined profiles of  $D$  and  $v$  are shown in figure 3. Calculating weighted residuals from the simulation of central SXR, Ni XVII 249Å and SXR profiles, simulation and experiment agree within ~15%.

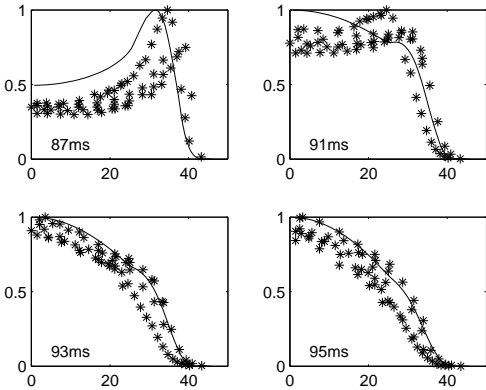


Figure 2: Reconstructed experimental SXR profiles (\*) for #26607 and their simulations.

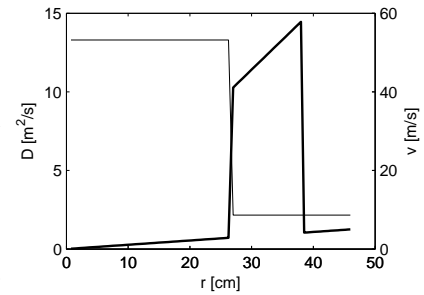


Figure 3: Profiles of  $D$  and  $v$  used in the QSH case simulation.

A significant feature is that  $v$  is directed outward over the whole plasma with an increased velocity barrier in the outer part of the plasma. This velocity opposes the penetration of Ni particles into the plasma core causing the Ni to remain mainly near the edge. Results from the SXR inversion confirm this with the initial edge peak due to Ni decaying without progressing into the core.

A further feature of the profiles is that the low  $D$ , good confinement, region at the edge extends over nearly half of the plasma. This is a change from previous results for C and O in lower plasma current [3] where the low  $D$  region at the edge was much smaller.

A simple variation test shows that the presence of a barrier in  $v$  gives better consistency than simulations omitting the barrier or with an edge reversal (inflow). Similarly the transition in  $D$  should be located at the barrier, however, some uncertainty as to the exact values of  $D$  and  $v$  remains.

**Ni transport in MH** Other discharges were obtained with LBO during different phases of QSH and in MH conditions. The latter case is illustrated in figures 4 and 5 where the

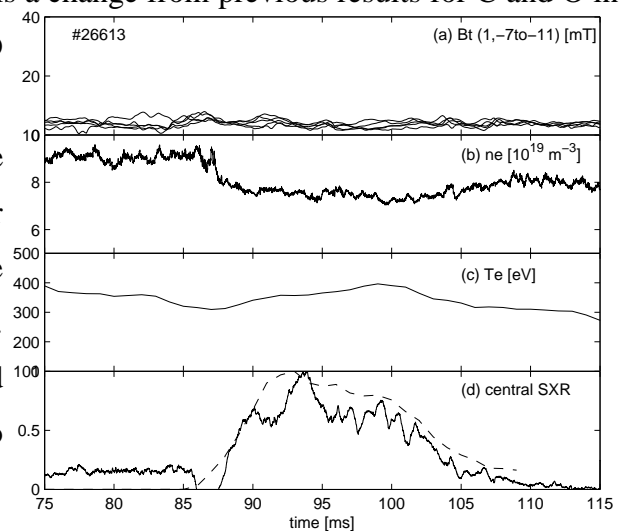


Figure 4: Discharge #26613 (1.3MA, LBO at 85ms): (a) Bt  $m=1$ ,  $n=-7$  to  $-11$ ; (b)  $n_e$ ; (c)  $T_e$ ; (d) central chord SXR and simulation (dashed).

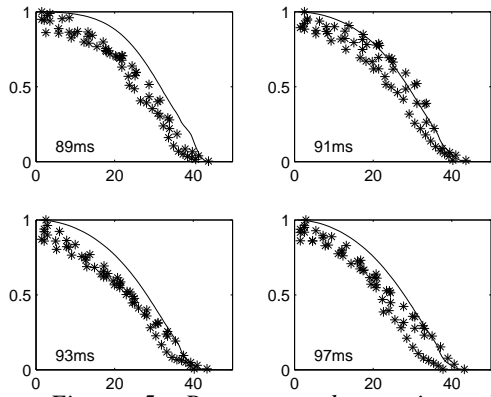


Figure 5: Reconstructed experimental SXR profiles (\*) for #26613 and their simulations.

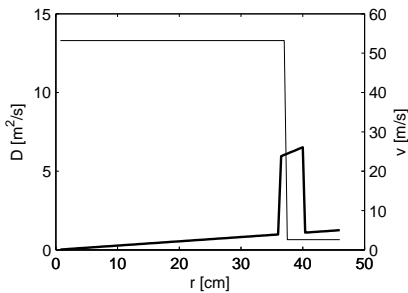


Figure 6: MH case  $D$  and  $v$ .

reconstructed SXR profiles immediately following the LBO are not hollow as in the QSH case. The central SXR and Ni line decays are slower – a 12ms time constant exponential decay compared to 8ms for the QSH case.

Different impurity transport coefficients as in figure 6 are needed. The main difference in the MH parameters is that the good confinement edge region does not extend as far into the plasma. The velocity barrier is weaker and is also shifted outwards. The more external D transition in MH is likely reflective of the different Te profile – figure 7 – which is flat to a large radius and then drops rapidly; in the QSH case Te profile was more peaked.

The Ni total density profiles at steady-state have been calculated by extrapolating the best simulations of the QSH and MH cases, assuming in both cases constant Te and ne (as measured at LBO in the QSH discharge) and constant Ni influx. The profiles (figure 8) show that there is a very effective barrier to the Ni penetration in the QSH case whilst in MH the particle level is higher in the core and extends further out. The resulting SXR time evolutions are very alike suggesting the experimental differences may be partly due to the very different plasma parameters in the two cases. We plan to increase our understanding of this by extending our database of LBO discharges in the next campaign.

The experiments seem not to indicate a significant difference in the confinement in the core for the QSH with respect to the MH regime. For the main gas there are indications of better confinement inside the hot helical region. The different behaviour of the two species finds a correspondence in the Monte Carlo ORBIT code results which attribute the

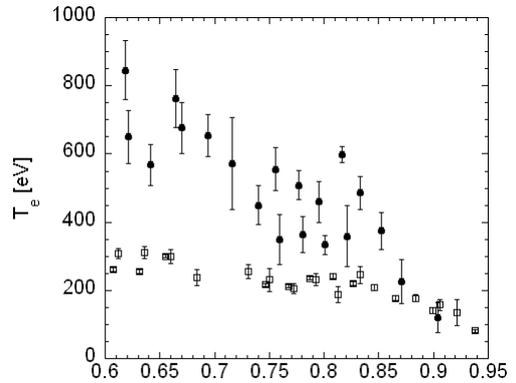


Figure 7: Edge  $T_e$  profile for #26607 (●) and #26613 (□).

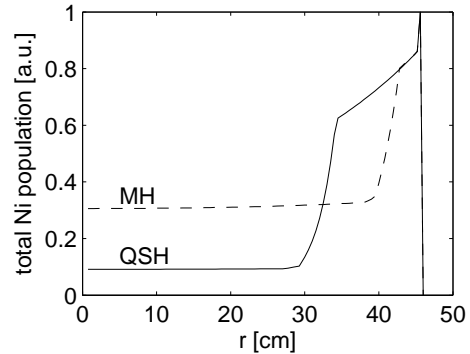


Figure 8: Stationary case total Ni population for QSH (full) and MH (dashed)  $D$  and  $v$ .

code results which attribute the

reproduction of the differences to the very different collisionalities [1,4]. At this moment there is only qualitative agreement with the ORBIT Ni results due to the order of magnitude difference in D obtained from experiment – more extensive analysis of this is ongoing.

**Ne impurity transport** Complementary experiments using neon gas puffing (figure 9) were also carried out at RFX-mod. Ne is a recycling impurity and so remains in the plasma

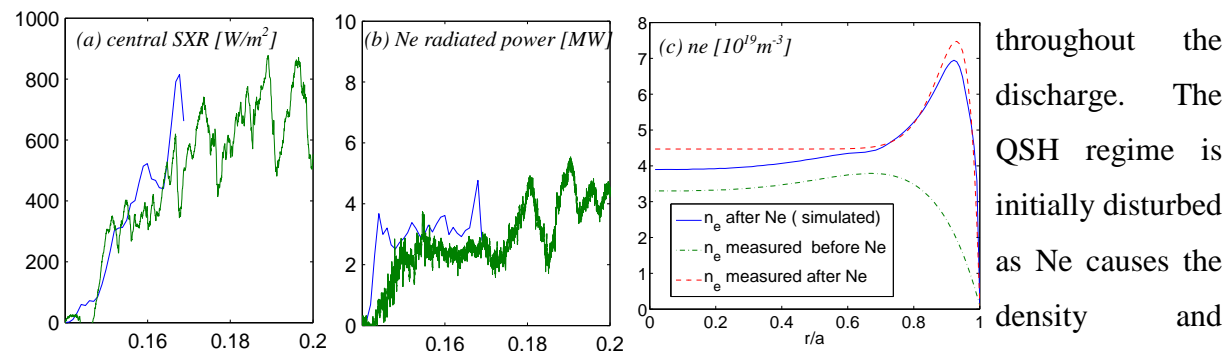


Figure 9: Discharge #26361, Ne puffing at 140ms: (a) central SXR; (b) Ne radiated power, both with simulation (blue); (c) time evolution of  $n_e$  profile

to climb, however, the typically intermittent QSH behaviour is quickly re-established. Using the Ni D and v from the QSH case above, we are able to reproduce the step increase in the SXR and radiated power signals. The density profile before and after the injection are reproduced. Ne is also confined in the edge region.

**Conclusions** The latest results of impurity transport analysis on RFX-mod are presented. Spectroscopic measurements from Ni laser blow-off and Ne puffing experiments were simulated with a 1-D impurity transport code. For Ni LBO into QSH the good confinement lower diffusion coefficient region at the edge extended further into the plasma than in previous analyses. An outward pinch velocity with large barrier in the external plasma and no reversal was found which acts strongly against Ni reaching the core. The transition region in D and v was determined to be closer to the edge for the MH plasma and the barrier weaker. The position of the barrier appears to be linked to that of the Te gradients. Particle transport and confinement seemed to be less influenced by the magnetic topology than by the plasma conditions of temperature and density. The Ni transport parameters of QSH regime were also able to reproduce the Ne transport within acceptable margins. That the same transport can be acceptable for both Ni and Ne impurities despite their mass difference suggests that we can also extend this to the intrinsic C and O impurities. In QSH the impurities do not accumulate.

**Acknowledgement** This work was supported by the European Communities under the contract of Associations between EURATOM/ENEA. One of the authors (S.M.) gratefully acknowledges the financial support from Vetenskapsrådet.

**References** [1] Carraro et al., Nuclear Fusion 49 (2009) 055009 [2] Mattioli et al., PPCF 44 (2002) 33 [3] Carraro et al., 33<sup>rd</sup> EPS Conf. Rome (2006) P5.083 [4] Carraro et al., IAEA (2008) EX/P3-9